Highly-efficient Cas9-mediated transcriptional programming

HHS Public Access

Author manuscript

Nat Methods. Author manuscript; available in PMC 2015 October 01.

Published in final edited form as:

Nat Methods. 2015 April ; 12(4): 326–328. doi:10.1038/nmeth.3312.

Highly-efficient Cas9-mediated transcriptional programming

Alejandro Chavez[1,2,3,10], **Jonathan Scheiman**[1,3,10], **Suhani Vora**[1,3,4,10], **Benjamin W. Pruitt**[1], **Marcelle Tuttle**[1], **Eswar Iyer**[1,3], **Shuailiang Lin**[3,5], **Samira Kiani**[4,6], **Christopher D. Guzman**[1], **Daniel J. Wiegand**[1], **Dmitry Ter-Ovanesyan**[1,3], **Jonathan L. Braff**[1], **Noah Davidsohn**[1,3], **Benjamin E. Housden**[3], **Norbert Perrimon**[3,5], **Ron Weiss**[4,6], **John Aach**[3], **James J. Collins**[1,7,8,9], and **George M. Church**[1,3]

[1]Wyss Institute for Biologically Inspired Engineering, Harvard University, Cambridge, MA 02138, USA

[2]Department of Pathology, Massachusetts General Hospital, Boston, MA 02114, USA

[3]Department of Genetics, Harvard Medical School, Boston, MA 02115, USA

[4]Department of Biological Engineering, Massachusetts Institute of Technology, Cambridge, MA 02139, USA

[5]Howard Hughes Medical Institute, Harvard Medical School, Boston, MA 02115, USA

[6]Synthetic Biology Center, Massachusetts Institute of Technology, Cambridge, MA 02139, USA

[7]Institute for Medical Engineering & Science, Department of Biological Engineering, Boston University, Boston, MA 02215, USA

[8]Synthetic Biology Center, Massachusetts Institute of Technology, Cambridge, MA 02139, USA

[9]Broad Institute of Massachusetts Institute of Technology and Harvard, Cambridge, MA 02142, USA

The RNA-guided nuclease Cas9 can be reengineered as a programmable transcription factor. However, modest levels of gene activation have limited potential applications. We describe an improved transcriptional regulator through the rational design of a tripartite activator, VP64-p65-Rta (VPR), fused to nuclease-null Cas9. We demonstrate its utility in activating endogenous coding and non-coding genes, targeting several genes simultaneously and stimulating neuronal differentiation of human induced pluripotent stem cells (iPSCs).

Correspondence should be addressed to G.M.C. (gchurch@genetics.med.harvard.edu).

[10]These authors contributed equally to this work

Competing Financial Interests:

G.M.C. is a founding member of Editas Medicine, a company that applies genome editing technologies.

Author Contributions:

A.C. and J.R.S. conceived of the study. A.C., J.R.S., and S.V. designed, performed experiments and interpreted data. B.P. designed and developed fusion libraries. M.T., D.T-O., C.D.G., D.J.W., performed experiments. N.D. and J.L.B. developed reagents. E.I. performed the iNeuron image analysis. S.K. and R.W. designed, tested and analyzed the TALE activator data. S.L., B.E.H., and N.P. designed, tested and analyzed S2R+ cells experiments. J.A. designed a subset of the gRNAs. J.J.C and G.M.C. supervised the study. A.C., J.R.S., S.V. and B.P. wrote the manuscript with support from M.T. and all other authors.

Cas9 is an RNA-guided endonuclease that is directed to a specific DNA sequence through complementarity between the associated guide RNA (gRNA) and its target locus[1,2]. Cas9 can be directed to nearly any arbitrary sequence with a gRNA, requiring only a short protospacer adjacent motif (PAM) site proximal to the target[3–5]. Through mutational analysis, variants of Cas9 have been generated that lack endonucleolytic activity but retain the capacity to interact with DNA[2,6,7]. These nuclease-null (dCas9) variants have been subsequently functionalized with effector domains such as transcriptional activation domains (ADs), enabling Cas9 to serve as a tool for cellular programming at the transcriptional level[6,8–10]. The ability to program the robust induction of expression at a specific target within its native chromosomal context would provide a transformative tool for myriad applications, including the development of therapeutic interventions, genetic screening, activation of endogenous and synthetic genetic circuits, and the induction of cellular differentiation[11–13].

In natural systems, transcriptional initiation occurs through the coordinated recruitment of necessary machinery by a number of locally concentrated transcription factor activation domains (ADs). As a result, we hypothesized that the tandem fusion of multiple ADs would increase transcriptional activation by mimicking the natural cooperative recruitment process. Towards this goal a series of more than 20 candidate effectors with known transcriptional roles were fused to the C terminus of *Streptococcus pyogenes* (SP)-dCas9, and their potency was assessed by a fluorescent reporter assay performed in human HEK 293T cells (Supplementary Figs. 1 and 2)[14].

Of the hybrid proteins tested, dCas9-VP64, dCas9-p65, and dCas9-Rta showed the most meaningful reporter induction. Nonetheless, neither the p65 nor the Rta hybrids were stronger activators than the commonly used dCas9-VP64 protein. Taking dCas9-VP64 as a starting scaffold, we subsequently extended the C-terminal fusion with the addition of either p65 or Rta. As predicted, these bipartite fusions exhibited increased transcriptional activity. Further improvement was observed when both p65 and Rta were fused in tandem to VP64, generating a hybrid VP64-p65-Rta tripartite activator (hereon referred to as VPR) (Supplementary Fig. 3).

To begin characterizing VPR, we verified the importance of each of its constituent domains (VP64, p65, and Rta) by replacing the respective member with mCherry, and measuring the resulting protein's activity by reporter assay. All fusions containing mCherry exhibited decreased activity, demonstrating the essentiality of all three domains (Supplementary Fig. 4). We further validated the importance of domain order by shuffling the positions of the three domains, generating all possible non-repeating dCas9 fusion proteins. Evaluation of the VPR permutations confirmed that the original ordering was indeed optimal (Supplementary Fig. 5).

Given the potency of our SP-dCas9-VPR fusion, we investigated whether the VPR construct would exhibit similar potency when fused to other DNA-binding scaffolds. Fusion of VPR to a nuclease-null *Streptococcus thermophilus* (ST1)-dCas9, a designer transcription activator like effector (TALE), or a zinc-finger protein allowed for an increase in activation relative to VP64 (Supplementary Fig. 6)[15].

Having performed initial characterization of our SP-dCas9-VPR fusion, we sought to assess its ability to activate endogenous coding and non-coding targets relative to VP64. To this end, we constructed three to four gRNAs against a set of factors related to cellular reprogramming, development, and gene therapy. When compared to the dCas9-VP64 activator, dCas9-VPR showed 22 to 320 fold improved activation of endogenous targets (Fig. 1A). While VPR was able to induce each of our target genes to a much greater extent than VP64, a marked difference in the relative levels of gene induction between targets was observed. Furthermore, in accordance with previous studies[16], we noted an inverse correlation between basal expression level and relative expression gain induced by dCas9 activators (genes with high basal expression were less potently activated) (Supplementary Fig. 7).

To place our observed levels of activation within a biologically relevant context we compared dCas9-VPR activation in HEK 293T cells with the expression of the same gene within its native human tissue. Absolute comparisons in gene expression between *in vitro* cell lines and native tissues are difficult, but our preliminary analysis suggests that we were able to activate a number of our target genes to similar levels as in their native tissues (Supplementary Fig. 8).

Cas9 enables multiplexed activation through the simple introduction of a collection of guide RNAs against a desired set of genes. To determine the efficiency of multi-gene targeting, we performed a pooled activation experiment simultaneously inducing four of our initially characterized genes: *MIAT*, *NEUROD1*, *ASCL1*, and *RHOXF2*. VPR allowed for robust multi-locus activation, exhibiting several-fold higher expression levels than VP64 across the panel of genes (Fig. 1B).

After demonstrating dCas9-VPR's ability to robustly activate gene expression in human cells, we sought to further explore its versatility as a general tool for gene induction within alternate model systems. Expression of dCas9-VPR in *Saccharomyces cerevisiae*, *Drosophila melanogaster* S2R+ cells, and *Mus musculus* Neuro-2A cells led to a range of improved activation from 5 to 300 fold over VP64 based activators (Supplementary Fig. 9).

The ability to selectively upregulate gene expression provides a powerful means to reprogram cellular identity for regenerative medicine and basic research purposes. Previous work has shown that the ectopic expression of several cDNAs promotes the differentiation of stem cells into multiple cell types. While such artificial induction often requires multiple factors, it was recently shown that exogenous expression of single transcription factors, Neurogenin2 (NGN2) or Neurogenic differentiation factor 1 (NEUROD1), is sufficient to promote differentiation of human iPS cells into induced neurons (iNeurons)[17,18]. While our previous attempts to generate iNeurons from iPS cells using dCas9-VP64-based activators were unsuccessful (data not shown), we were optimistic that the increased potency of VPR might induce sufficient expression of NGN2 and/or NEUROD1 protein to trigger differentiation.

Stable PGP1 iPS, doxycycline-inducible, dCas9-VP64 and dCas9-VPR cell lines were generated and transduced with lentiviral vectors containing a mixed pool of 30 gRNAs

directed against either *NGN2* or *NEUROD1*. To determine differentiation efficiency, gRNA containing dCas9-AD iPS cell lines were cultured in the presence of doxycycline and monitored for phenotypic changes (Supplementary Figs. 10 and 11). We observed that VPR, in contrast to VP64, enabled rapid and robust differentiation of iPS cells into a neuronal phenotype. Additionally, these cells stained positively for the neuronal markers beta III tubulin and neurofilament 200 (Fig. 2A and Supplementary Fig. 12A, respectively). Subsequent quantification of the staining revealed that dCas9-VPR cell lines showed a 10 to 37-fold improvement in the amount of iNeurons observed through upregulation of either NGN2 or NEUROD1 (Fig. 2B and Supplementary Fig. 12B). Analysis by qRT-PCR revealed a 10-fold and 18-fold increase in *NGN2* and *NEUROD1* mRNA expression levels, respectively, within dCas9-VPR cells over their dCas9-VP64 counterparts (Fig. 2C).

Over the past year there were a number of exciting advances in the field of Cas9-derived transcriptional activators. Two-component systems that rely on innovative gRNA modifications (e.g., synergistic activation mediator (SAM) and scaffold RNA (scRNA)) and epitope-based attachment systems (e.g., SUperNova (SunTag)) continue to push the limits of activator potency[16,19,20]. Notably, it was shown that the multimeric recruitment of even modestly effective activation domains (i.e., VP64 and p65) can lead to abundant increases in transcriptional output[16,19,20]. We believe that the rational selection and ordered fusion of individual activator domains provides an approach that is highly effective while eliminating the delivery and design complications generated by a two-component activator. In addition, as even modestly potent activation domains have exhibited marked improvement in activity when repeatedly recruited to a single dCas9 protein, we envision that our more potent VPR activator should lead to drastically improved activation if multiply recruited to a single dCas9 protein through technologies such as SAM, scRNA or SunTag.

Beyond the utility of VPR as a technological catalyst, we believe that our design process brings to light several important generalizations for future synthetic effectors, most notably the importance in screening large numbers of putative candidates and the critical role of domain order in the emergent synergy of multi-component fusions.

Online Materials and Methods

Vectors used and designed

Activation domains were cloned using a combination of Gibson and Gateway assembly or Golden Gate assembly methods. For experiments involving multiple activation domains, ADs were separated by short glycine-serine linkers. Activator sequences are listed in the Supplementary Data (vectors to be deposited in Addgene). All SP-dCas9 plasmids were based on Cas9m4-VP64 (Addgene #47319)[6], ST1-dCas9 plasmids were based on M-ST1n-VP64 (Addgene #48675)[15]. Sequences for gRNAs are listed in the supplementary information. gRNAs for endogenous human gene activation were selected to bind between 1 and 1000 bp upstream of the transcriptional start site (TSS). gRNAs for iPSC differentiation to iNeurons, targeting *NGN*2 and *NEUROD1*, were selected to bind between 1 and 2000 base pairs upstream of the transcriptional start site. All human gRNAs were expressed from either cloned plasmids (Addgene #41817)[5] or integrated into the genome through lentiviral

delivery (plasmid SB700). Guide RNA sequences are listed within the Supplementary Data. Reporter targeting gRNAs were previously described (Addgene #48671 and #48672)[6].

Mammalian cell culture and transfections

HEK 293T cells (gift from P. Mali, UCSD) and Neuro-2A cells (ATCC CCL-131), were maintained in high glucose Dulbecco's Modified Eagle's Medium (Invitrogen) supplemented with 10% FBS (Invitrogen) and penicillin/streptomycin (Invitrogen). Cells were maintained at 37°C and 5% CO_2 in a humidified incubator and tested for mycoplasma yearly. Cells were transfected in 24-well plates seeded with 50,000 cells per well. 200ng of dCas9 activator, 10ng of gRNA and 60ng of reporter plasmid (when required) were delivered to each well with Lipofectamine 2000 (HEK 293T) or Lipofectamine 3000 (Neuro-2A), according to manufacturer's instructions. For multiplex activation, a 40ng mix of gRNAs was used, with a 10ng total amount of guide per each of the four gene targets. For example, if four guide RNAs were used against an individual target, 2.5ng of each guide RNA were combined, to obtain a 10ng mix for that target - then the four 10ng mixes were combined to prepare 40 ng total for transfection. Cells were grown 36–48 hours after transfection before being assayed using fluorescence microscopy, flow cytometry or lysed for RNA purification and quantification.

S. cerevisiae manipulation

Yeast strain W303 was used for all experiments. dCas9 activator constructs were cloned into vector pAG414-GPD (Addgene #14144)[21]. gRNAs (located between 100–200 bp upstream of the TSS) were expressed from the SNR52 promoter and cloned into the 2μ based pAG60-2u vector[22]. Cells were grown up overnight at 30°C in synthetic complete media lacking tryptophan and uracil. The following day cells were diluted 1:100 into 5mls of fresh media and grown for an additional 7 hours at 30°C. 2mls of culture was then spun down for RNA extraction.

Drosophila culture

Drosophila S2R+ cells were grown in Schneider's medium (Invitrogen) supplemented with 10% heat-inactivated FBS (JRH Biosciences) and penicillin/streptomycin (Sigma) at 25°C without CO_2. Cells were transfected using Effectene Transfection Reagent (Qiagen) according to manufacturer's instructions. Transfections were performed in 24 well plates and cells were seeded at 30,000 cells per well. 150ng of dCas9 activator and 50ng gRNAs were transfected and incubated for 3 days at 25°C before extraction of total RNA. Five gRNAs were transfected against each of the indicated target genes.

Fluorescence Reporter Assay

SP-dCas9 reporter assays were performed by targeting all dCas9-ADs with a single guide to a minimal CMV promoter, driving expression of a fluorescent reporter. Addgene plasmid #47320[6] was used to screen for novel ADs (Supplementary Figs. 1 and 2) or was altered to contain a sfGFP reporter gene instead of tdTomato (Supplementary Figs. 3B, 4 and 5). In addition, to control for transfection efficiency (Supplementary Figs. 3B, 4 and 5) an EBFP2 expressing control plasmid was co-transfected at 25ng per well (EBFP2 plasmid was not co-

transformed in Supplementary Fig. 2). To remove untransfected cells from the analysis, sfGFP fluorescence was only analyzed in cells with $>10^3$ EBFP2 expression (as determined by flow cytometry). For fusion of VPR to other programmable transcription factors (ST1-dCas9, TALE, and zinc-finger protein) no EBFP2 plasmid was transfected. ST1-dCas9 reporter assays were performed using the previously described tdTomato reporter with an appropriate PAM inserted upstream of the tdTomato coding region (Addgene #48678)[15]. The binding sequences for the zinc finger and TALE are TAATTANGGGNG and ACCTCATCAGGAACATGTT, respectively.

qRT-PCR analysis

Yeast RNA was extracted using the YeaStar kit (Zymogen), RNA from *Drosophila* S2R cells was extracted using Trizol (Life Technologies), and RNA from human cells was extracted using the RNeasy PLUS mini kit (Qiagen). Human tissue RNA was obtained from Life Technologies (Human Brain Total RNA (AM7962), Human Heart Total RNA (AM7966) and Human Testes Total RNA (AM7972)). 500ng of RNA was used with the iScript cDNA synthesis Kit (BioRad), and 0.5μl of cDNA was used for each qPCR reaction, utilizing the KAPA SYBR® FAST Universal 2X qPCR Master Mix. The *Drosophila* qPCR reaction used iQ SYBR. qPCR primers are listed within the Supplementary Table 1. qRT-PCR was run and analyzed on the CFX96 Real-Time PCR Detection System (BIORAD), with all target gene expression levels normalized to β-actin mRNA levels (human and *M. musculus*), *FBA1* mRNA levels (*S. cerevisiae*) or RpL32 mRNA levels (*D. melanogaster*).

Lentivirus production

Lentiviral particles were generated by transfecting 293T cells with the pSB700 sgRNA expression plasmid (with cerulean reporter) and the psPAX2 & pMD2.G (Addgene #12260 and #12259) packaging vectors at a ratio of 4:3:1, respectively. Viral supernatants were collected 48–72h following transfection and concentrated using the PEG Virus Precipitation Kit (BioVision) according to the manufacturer's protocol.

iPSC culture and dCas9-AD cell line generation

PGP1 iPS cells were obtained from the Coriell Institute Biorepository (GM23338) and maintained on matrigel (Corning) coated tissue culture plates in mTeSR1 Basal medium (Stemcell technologies). To generate stable iPS dCas9-AD expressing cell lines, approximately 5x10^5 cells were nucleofected with 1.5μg of dCas9-AD piggy-bac expression vector and 340ng of transposase vector (System Biosciences) using the Amaxa P3 Primary Cell 4D-Nucleofector X Kit (Lonza), program CB-150. Following electroporation, cells were seeded onto 24-well matrigel-coated plates in the presence of 10uM ROCK inhibitor (R&D systems) and allowed to recover for two days before expanding to 6-well plates in the presence of 20ug/ml hygromycin to select for a mixed population of dCas9-AD integrant containing cells.

iPSC transduction and neural induction

iPS dCas9-AD cell lines were transduced with lentiviral preparations containing 30 gRNAs, targeted against either *NEUROD1* or *NGN2*, one day after seeding onto matrigel coated

plates. Transduced cells were expanded and then sorted for the top 15% of cerulean positive cells (pSB700 gRNA expression). Sorted gRNA containing dCas9-AD iPS cell lines were seeded in triplicates onto matrigel coated 24-well plates with mTeSR + 10uM ROCK inhibitor, either in the presence or absence of 1ug/ml of doxycycline. Fresh mTeSR medium + or − doxycycline was added every day for 4 days, at which cells were analyzed by light microscopy, immunofluorescence and harvested for qRT-PCR analysis.

Immunostaining of Cas9 iNeurons

All steps for staining were performed at room temperature. Samples were washed once with PBS then fixed with 10% formalin (Electron Microscopy Sciences) for 20 min followed by permeabilization with 0.2% Triton X-100/PBS for 15 min. Samples were then blocked with 8% BSA for 30 min followed by staining with primary antibodies diluted into 4% BSA. Staining was performed for either 3h with anti-beta III eFluor 660 conjugate (eBioscience, catalog no. 5045-10, clone 2G10-TB3) or 1h with anti-neurofilament 200 (Sigma, catalog no. N4142), both at a 1:500 dilution. Samples were then washed 3 times, 5 minutes each, with 0.1% tween/PBS, followed by one wash with PBS. For neurofilament 200 staining, a secondary donkey anti-rabbit Alexa Fluor 647 (Life Sciences) antibody was added at a 1:1000 dilution in 4% BSA for 1h. Samples were again washed as previously mentioned then stained with nucBlue [Hoechst 33342] (Life Sciences) for 5 min.

Image acquisition and analysis of Cas9 iNeurons

24-well plates stained for NucBlue and neuronal markers, were imaged with a 10x objective on a Zeiss Axio Observer Z1 microscope. Zen Blue software (Zeiss) was used to program acquisition of 24 images per well. Total cell (NucBlue) and iNeuron (Beta III tubulin or Neurofilament 200) counts were quantified for each image using custom Fiji and Matlab scripts and used to determine the percentage of iNeurons per well by the formula: (number of Beta III positive cells/number of nucBlue cells) × 100. In preparation for publication, individual channels were composited and pseudocolored, with equal adjustments across samples and controls, in Fiji.

Statistical analysis

All statistical comparisons are two-tailed t-tests calculated using the GraphPad Prism software package (Version 6.0 for Windows. GraphPad Software, San Diego, CA). All sample numbers listed indicate the number of biological replicates employed in each experiment.

Code availability

Custom Fiji and Matlab scripts utilized in analyzing iPS cell differentiation are available upon request.

Reproducibility

Throughout our study, we employ a sample size which is frequently used for similar kinds of experiments. No data were excluded from any of our analysis. No randomization was

employed and blinding was not used except in iNeuron image analysis where the scientist quantifying each of the conditions was blind to the sample type.

Supplementary Material

Refer to Web version on PubMed Central for supplementary material.

Acknowledgments

We thank K. Esvelt, P. Mali and the rest of the members of the Church and Collins labs for helpful discussions. We thank T. Ferrante, S. Byrne and M. Farrell for technical assistance, A. Keung (Massachusetts Institute of Technology) for providing zinc-finger reporter constructs, and J. Schulak for graphic design. This work was supported by US National Institutes of Health NHGRI grant P50 HG005550, US Department of Energy grant DE-FG02-02ER63445 and the Wyss Institute for Biologically Inspired Engineering. A.C. acknowledges funding by the National Cancer Institute grant 5T32CA009216-34. S.V. acknowledges funding by the National Science Foundation Graduate Research Fellowship Program, the Department of Biological Engineering at MIT, and the Department of Genetics at Harvard Medical School.

References

1. Garneau JE, et al. The CRISPR/Cas bacterial immune system cleaves bacteriophage and plasmid DNA. Nature. 2010; 468:67–71. [PubMed: 21048762]
2. Jinek M, et al. A programmable dual-RNA-guided DNA endonuclease in adaptive bacterial immunity. Science. 2012; 337:816–821. [PubMed: 22745249]
3. Mojica FJM, Díez-Villaseñor C, García-Martínez J, Almendros C. Short motif sequences determine the targets of the prokaryotic CRISPR defence system. Microbiol Read Engl. 2009; 155:733–740.
4. Cong L, et al. Multiplex genome engineering using CRISPR/Cas systems. Science. 2013; 339:819–823. [PubMed: 23287718]
5. Mali P, et al. RNA-guided human genome engineering via Cas9. Science. 2013; 339:823–826. [PubMed: 23287722]
6. Mali P, et al. CAS9 transcriptional activators for target specificity screening and paired nickases for cooperative genome engineering. Nat Biotechnol. 2013; 31:833–838. [PubMed: 23907171]
7. Sapranauskas R, et al. The Streptococcus thermophilus CRISPR/Cas system provides immunity in Escherichia coli. Nucleic Acids Res. 2011; 39:9275–9282. [PubMed: 21813460]
8. Gilbert LA, et al. CRISPR-mediated modular RNA-guided regulation of transcription in eukaryotes. Cell. 2013; 154:442–451. [PubMed: 23849981]
9. Maeder ML, et al. CRISPR RNA-guided activation of endogenous human genes. Nat Methods. 2013; 10:977–979. [PubMed: 23892898]
10. Perez-Pinera P, et al. RNA-guided gene activation by CRISPR-Cas9-based transcription factors. Nat Methods. 2013; 10:973–976. [PubMed: 23892895]
11. Mali P, Esvelt KM, Church GM. Cas9 as a versatile tool for engineering biology. Nat Methods. 2013; 10:957–963. [PubMed: 24076990]
12. Hsu PD, Lander ES, Zhang F. Development and Applications of CRISPR-Cas9 for Genome Engineering. Cell. 2014; 157:1262–1278. [PubMed: 24906146]
13. Gersbach CA. Genome engineering: the next genomic revolution. Nat Methods. 2014; 11:1009–1011. [PubMed: 25264777]
14. Poss ZC, Ebmeier CC, Taatjes DJ. The Mediator complex and transcription regulation. Crit Rev Biochem Mol Biol. 2013; 48:575–608. [PubMed: 24088064]
15. Esvelt KM, et al. Orthogonal Cas9 proteins for RNA-guided gene regulation and editing. Nat Methods. 2013; 10:1116–1121. [PubMed: 24076762]
16. Konermann S, et al. Genome-scale transcriptional activation by an engineered CRISPR-Cas9 complex. Nature. 2015; 517:583–588. [PubMed: 25494202]
17. Busskamp V, et al. Rapid neurogenesis through transcriptional activation in human stem cells. Mol Syst Biol. 2014; 10:760. [PubMed: 25403753]

18. Zhang Y, et al. Rapid Single-Step Induction of Functional Neurons from Human Pluripotent Stem Cells. Neuron. 2013; 78:785–798. [PubMed: 23764284]

19. Tanenbaum ME, Gilbert LA, Qi LS, Weissman JS, Vale RD. A protein-tagging system for signal amplification in gene expression and fluorescence imaging. Cell. 2014; 159:635–646. [PubMed: 25307933]

20. Zalatan JG, et al. Engineering Complex Synthetic Transcriptional Programs with CRISPR RNA Scaffolds. Cell. 2015; 160:339–350. [PubMed: 25533786]

21. Alberti S, Gitler AD, Lindquist S. A suite of Gateway® cloning vectors for high-throughput genetic analysis in Saccharomyces cerevisiae. Yeast. 2007; 24:913–919. [PubMed: 17583893]

22. DiCarlo JE, et al. Genome engineering in Saccharomyces cerevisiae using CRISPR-Cas systems. Nucleic Acids Res. 2013; 41:4336–4343. [PubMed: 23460208]

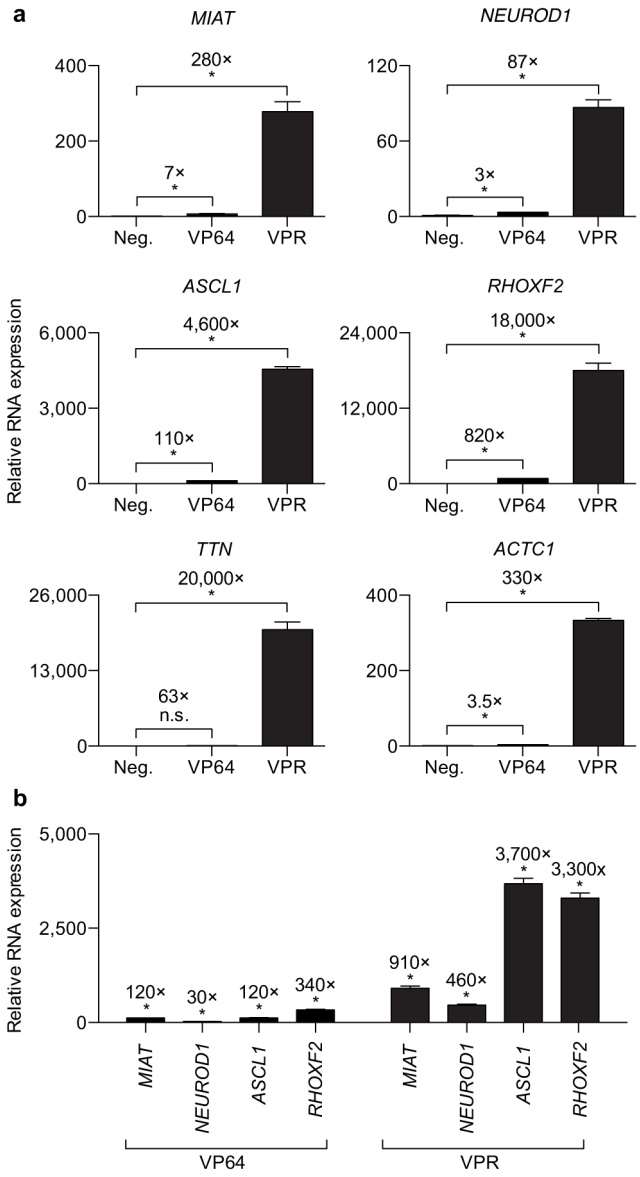

Figure 1.

Gene activation using VPR. (**a**) RNA expression of individual targets in HEK 293T cells transfected simultaneously with three or four gRNAs targeting the indicated genes along with the labeled dCas9-activator construct. Negative controls (Neg.) were transfected with indicated guide RNAs alone. Data are shown as the mean ± s.e.m (n = 3 independent transfections). For *, P = < 0.05 (n.s. = not significant). Comparison of dCas9-VP64 vs. dCas9-VPR, for all genes, is significant (P = <0.0011). (**b**) RNA expression during multiplex activation of the indicated four endogenous gene targets. Data are shown as the mean ± s.e.m (n = 3 independent transfections). For *, P = < 0.05. Comparison of dCas9-VP64 vs. dCas9-VPR, for all genes, is significant (P = <0.0022).

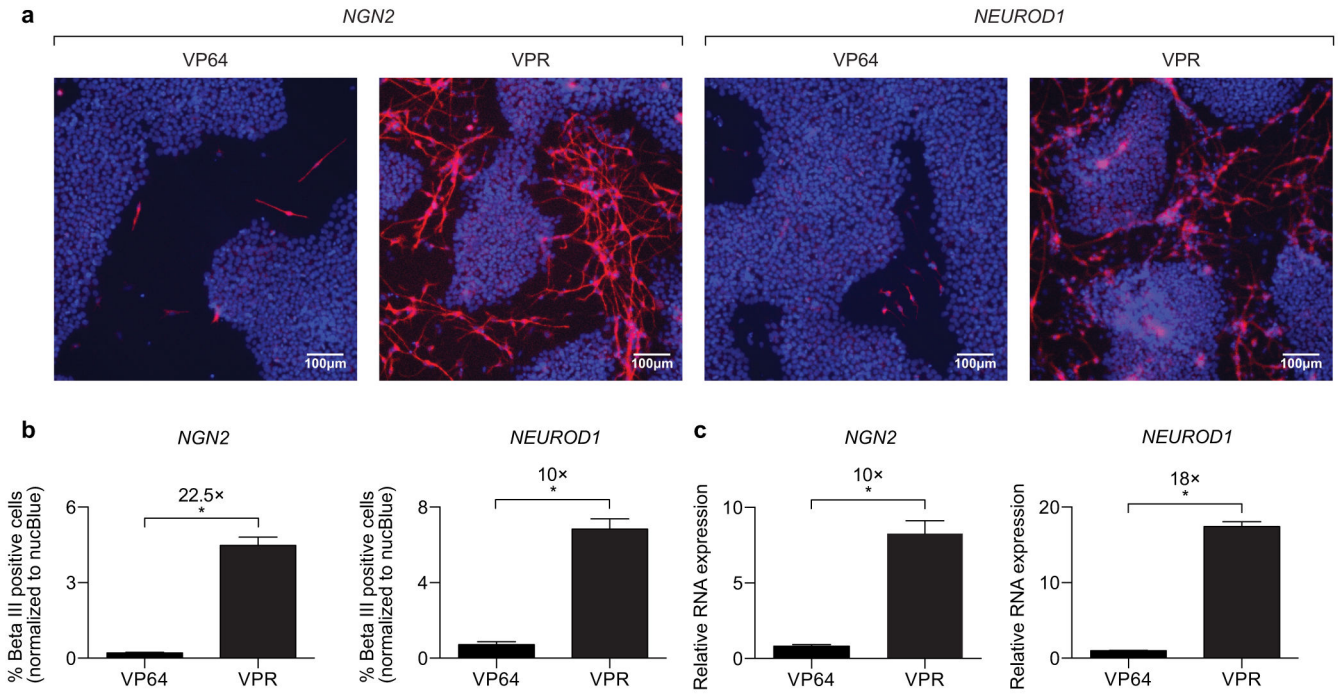

Figure 2.

dCas9-mediated iPSC neuronal differentiation using VPR. (**a**) Pseudocolored immunofluorescence images for NucBlue (blue, total cells) and beta III tubulin (red, iNeurons) four days after doxycycline induction. Images are representative of biological triplicates (separately seeded wells). Scale bar represents 100 μm. (**b**) Immunofluorescence quantification and comparison of iNeurons generated by either dCas9-VP64 or dCas9-VPR. Data is shown as the mean ± s.e.m. (n = 3 independent platings of stable cell lines, with each replicate being an average of 24 separate images). For *, P = < 0.001. (**c**) qRT-PCR analysis of mRNA expression levels of *NGN2* and *NEUROD1* in dCas9-AD iPS cell lines. Data is normalized to dCas9-VP64 cells and shown as the mean ± s.e.m. (n = 2 independent platings of each stable cell line). For *, P = < 0.05.